Propeller Noise at Model- and Full-Scale

W.J.G. Trebble* and J. Williams†
Royal Aircraft Establishment, Farnborough, Hampshire, Great Britain
and
R.P. Donnelly‡
Dowty-Rotol Limited, Cheltenham, Great Britain

As part of the aeroacoustic research at RAE on aircraft propellers, experiments have been completed on a Dowty-Rotol four-bladed R292 propeller (ARA-D section), at full-scale in the 24-ft anechoic tunnel and at quarter-scale on a geometrically similar model in the 1.5-m acoustic tunnel. Measurements were made of power, torque, and thrust, simultaneously with microphone recording of the propeller noise signal. Analysis of the third-octave and narrow-band spectra are presented for a range of rotational speeds up to a blade-tip Mach number of 0.75, for an extensive range of blade-angle settings, with tunnel airspeeds up to 50 m/s. The quarter-scale model is shown to have closely similar acoustic and aerodynamic characteristics to those of the full-scale propeller. As expected, substantially better noise measurements proved attainable in the 1.5-m acoustic tunnel than in the 24-ft anechoic tunnel, though perforce at smaller scale. The relevance of aerodynamic testing at airstream speeds approaching typical flight Mach numbers is also illustrated. Parametric formulas and fundamental theoretical frameworks for propeller noise prediction are discussed. While useful correlation is exhibited between the measured and predicted sound levels for the discrete tones, substantial discrepancies exist for the apparent broadband noise.

Introduction

IN recent years, there has been a renewal of interest in efficient subsonic propellers for the operation of quiet short-haul transports at moderate subsonic cruise speeds ($M = 0.25$-0.6), particularly in view of the rapid increase in fuel costs, the need for fuel conservation, and the demands for noise reduction. For modern turbo-prop aircraft the propeller itself may be regarded as the predominant noise source in respect of both ground-level and internal cabin effects. Although aircraft installation effects are significant, it was considered that a program of research on propeller noise should start by investigating isolated propellers in a wind tunnel at full- and model-scale.[1]

This paper reports experiments on a Dowty-Rotol four-bladed R292 propeller (ARA-D section) of 2.82 m diam, at full-scale in the 24-ft anechoic tunnel and at quarter-scale on a geometrically similar model in the 1.5-m acoustic tunnel. Measurements were made of aerodynamic power, torque, and thrust, simultaneously with microphone recording of the propeller noise signal. Third-octave and narrow-band noise spectra have been analyzed for a range of rotational speeds up to a blade-tip Mach number of 0.75, for an extensive practical range of blade-angle settings, with tunnel airspeeds up to 50 m/s. These research studies are intended to help establish and improve the range of validity of small-scale experimental models and of theoretical frameworks for the prediction of the noise characteristics and allied aerodynamic performance of isolated propellers—including possible new designs required to reduce further noise levels with negligible penalty on aerodynamic efficiency.

Full-Scale Wind Tunnel Techniques

The limitations of the 24-ft anechoic tunnel (Fig. 1), particularly in respect to high background noise much above 30 m/s airspeed and some reverberation problems well below 1 kHz, are well appreciated, but can be more tolerable for investigations involving intense discrete tones rather than broadband noise sources. As ancillary aerodynamic equipment, the large open-jet test section (7.3 m diam) has a quiet powered nacelle of 1.2 m diam and 4 m length, powered by a 1200-kW three-phase electric motor, specifically designed for driving medium-size propellers. Instrumentation includes precision watt-meters together with an accurate indication of rotational speed and slip, so that the true power output and revolutions per minute can be monitored. The existing nacelle-rig, mounted from the two-component lower-balance in the floor of the tunnel, allows thrust to be measured along the tunnel airstream axis, while lift arising from any nonaxisymmetric interactions or from the permissible tilting of the thrust axis can also be measured.

The experiments on the Dowty-Rotol four-bladed ARA-D propeller ($D_p = 2R = 2.82$ m) were made in March 1980, with rotational speeds varied up to 1700 rpm, with tunnel airspeeds restricted perforce from 10 to 50 m/s but through a wide range of blade-angle settings within safe operating limits. These tests aimed to cover the relevant range of blade-tip helical Mach number and aerodynamic incidence for takeoff and cruise. Near- and far-field noise studies have been carried out by microphones traversed linearly along the windstream direction, at distances of 1.77 and $4.17R$ from the propeller axis, ranging from a position $0.5R$ upstream of the propeller disk plane to about $2.0R$ downstream (Fig. 1).

Model-Scale Wind Tunnel Techniques

For research on propeller models in the 1.5-m acoustic tunnel, a new test-rig has been constructed (Fig. 2). The compact quiet drive is provided by a three-phase variable-frequency electric motor housed in a cylinder of 140 mm diam with a length of 400 mm. The long nacelle provides ample space for the installation of strain-gage links for the measurement of torque and thrust to complement tachometer readings of rotational speed. This motor was designed to be capable of producing over 70 Nm torque continuously at any rotational speed up to 10,000 rpm (i.e., a power of 75 kW at 10,000 rpm); preliminary evidence suggests that values of torque at least 20% above design should be available without the creation of excessive heating in this water-cooled motor.

Presented as Paper 81-2004 at the AIAA 7th Aeroacoustics Conference, Palo Alto, Calif., Oct. 5-7, 1981; submitted Oct. 13, 1981; revision received March 15, 1982.

*Member of Aerodynamics Department.
†Member of Aerodynamics Department.
‡Noise Engineer.

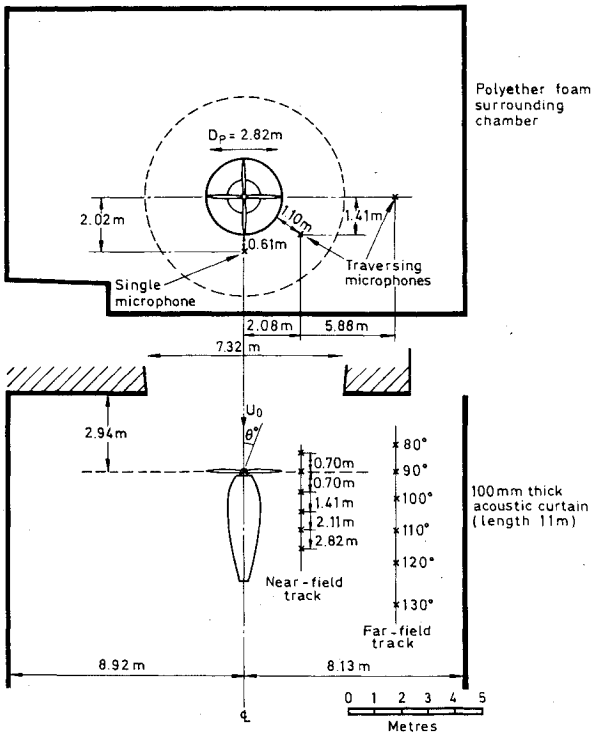

Fig. 1 Propeller and microphone installation in a 24-ft tunnel.

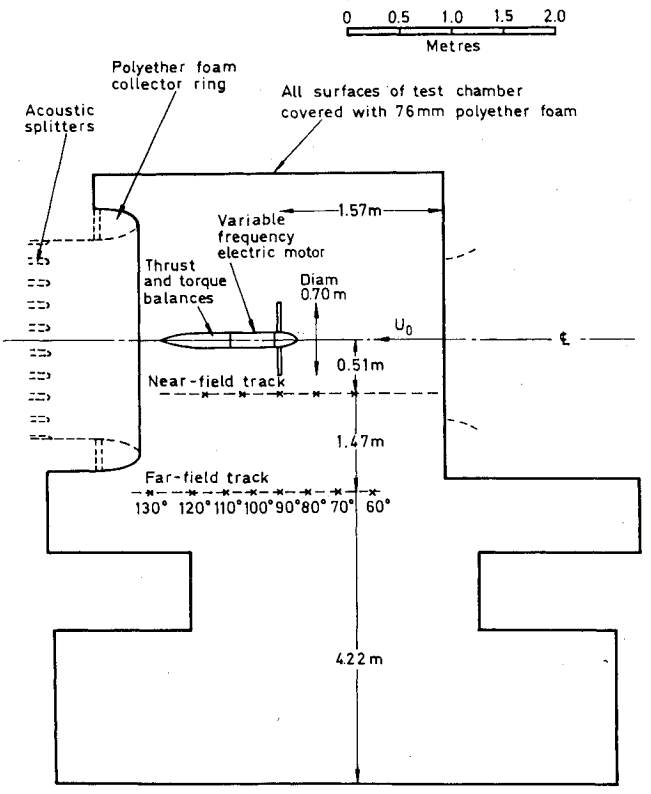

Fig. 2 Propeller model testing in a 1.5-m acoustic tunnel.

Consequently the unit has proved to be more than adequate to drive a fully representative quarter-scale model ($D_p = 0.7$ m) of the Dowty-Rotol ARA-D four-bladed propeller. The upper test limits have been solely determined by the propeller manufacturer's recommendation that torque should not exceed 75 Nm and that maximum permitted rotational speed should be limited to 8000 rpm. Rotational speeds between 4800 and 6800 rpm are here required to simulate the propeller-tip speed range experienced by the full-scale propellers on the aircraft. The nacelle axis can be inclined to the tunnel airstream direction (strictly rotation in yaw rather than pitch) and tests can be made at airspeeds up to 60 m/s.

Aeroacoustic research on this isolated propeller-nacelle in the 1.5-m acoustic tunnel (Fig. 2) uses noise measuring techniques similar to those for the 24-ft tunnel, as described below, but takes advantage of the greater flexibility and accessibility of the model and rig for more varied and rapid testing.

Acoustic Measurement and Analysis Techniques

Noise measurements were made using 6-mm condenser microphones traversed linearly, at distances of 1.77 and $4.17R$ from the propeller axis, to provide the array of near- and far-field positions illustrated in Figs. 1 and 2. The microphones inside the windstream were provided with ogival nose cones which were aligned directly into wind, while the microphones in the anechoic chamber outside the mainstream flow were provided with standard protective grills and their axes were directed normal to the tunnel centerline. The positioning of an additional microphone nearer to the propeller ($r/R = 1.44$) was chosen to give more correct representation of the distance between the propeller tip and the adjacent fuselage side of the Shorts 330 aircraft.

Signals from the microphones were fed through preamplifiers and measuring amplifiers to record on magnetic tape in a multichannel tape-recorder. For the full-scale propeller, this recorder was operated at 30 in./s to give good frequency response (±1 dB) for frequencies from 6 Hz to 20 kHz for both recording and replaying. However, for the quarter-scale model, propeller recordings were made at 60 in./s with replay at 15 in./s to effectively represent full-scale frequency on the read-out.

Acoustic treatment applied to the working-chamber boundary of the test section of the 24-ft tunnel provides an anechoic facility at frequencies in excess of some 300 Hz, but this is significantly higher than the blade-passing-frequency of these propeller tests, which varied between 67 and 113 Hz for rotational speeds of 1000-1700 rpm of the four-bladed propeller. The near-field microphone at 0.6 and 1.1 m from the propeller disk perimeter were close enough to the noise source for the acoustic signal received to be unaffected by boundary reflections; but the far-field microphone at 5.88 m from the tunnel centerline was only $\ell = 2.26$ m from the acoustic curtain (Fig. 1). It was therefore decided to check the anechoic properties at the far-field microphone using the tone-burst technique with a loudspeaker mounted on the tunnel centerline just ahead of the propeller. The results of this investigation indicate that the amplitude of the reflected signal was less than one-third of the incident signal at frequencies above 300 Hz, but at lower frequencies it increased to over half the amplitude of the incident signal, a value consistent with a perfect reflection at the acoustic curtain, taking the relative path lengths into consideration.

Thus, for *random noise*, the measured sound pressure level from the propeller at the far-field microphone should be reduced by 2 dB at frequencies below 300 Hz, but at higher frequencies the error rapidly reduces and becomes less than 0.2 dB above 800 Hz. Simple analysis of possible pressure signal interference effects for plane-wave pure tones (i.e., harmonics of the blade-passing frequency) suggests that these can vary significantly with wavelength. For these tests, errors could vary between a short fall of 6 dB (e.g., for the blade-passing frequency at 1700 rpm) to an excess of 3 dB if perfect correlation could be assumed between incident and reflected signals in this working environment. Even so, the relative effect of blade angle change would remain correctly represented in the measurements.

For the quarter-scale model in the 1.5-m tunnel, the increase in the relative size of the anechoic chamber alleviates any reflection problems. Some typical corrections are indicated later in the comparisons between full- and model-scale noise signals (Fig. 14).

At this stage no attempt has been made to allow specifically for the effects of either convection in the windstream or refraction through the jet mixing region on the acoustic signal measurements as a propeller forms such a relatively large and complex noise source. However, the magnitude of possible corrections to measurements along the far-field track ($r/R=4.17$) for noise emanating from a simple source on the tunnel centerline have been assessed using the method of Amiet.[2] Even at the extreme angular position ($\theta=130$ deg) and maximum test speed (50 m/s), where the corrections are greatest, they do not exceed an effective reduction of 5.5 deg in angle and 1 dB reduction in level.

Full-Scale Noise Spectra Analysis

Typical time histories of the acoustic signal received at 0.6 m from the blade tip are shown in Fig. 3 for a range of propeller rotational speed at a blade setting $\beta_{0.7}=21.5$ deg. The selected time period (0.08 s) is sufficient to represent a complete cycle of the propeller rotation even at the low rotational speed of 800 rpm and there does not appear to be any significant variation in the signal shape as each of the four blades passes the microphone in turn. At 800 rpm, the pressure response appears to be of a basically sinusoidal nature but the leading edge of the response curve steepens up as the rotational speed is increased. Then, between 1600 and 1700 rpm, there is a significant change with a very narrow peak in the pressure response curve suggesting the possibility of shock formation on the blade surface.

Samples of the one-third-octave noise spectra are presented for the near-field microphone position at 0.6 m from the propeller disk ($r/R=1.44$) in Figs. 4 and 5 and for the far-field microphone position at 4.46 m ($r/R=4.17$) in Fig. 6. There are increases in both the broadband noise and the tonal content with increase in either rotational speed or blade angle of the propeller. At moderate values of mainstream speed, the background noise of the tunnel and rig is sufficiently low for it to have little effect on the noise signatures from the propeller. However, at $U_0=50$ m/s (maximum speed) this background noise tends to obscure the propeller broadband spectra at frequencies below 5 kHz, though the propeller low-frequency tones are readily identified when the blades are operated at positive aerodynamic incidence—i.e., excluding low blade angle and low values of rotational speed.

Overall unweighted sound pressure levels (OASPL) and A-weighted levels are both available for the full range of tested propeller parameters. The OASPL (80 Hz to 20 kHz) for the near-field position are plotted against aerodynamic blade incidence ($\alpha^\circ_{0.85}$) at 85% radius in Fig.7. The noise level appears to be reasonably consistent with the relation

$$\text{OASPL}=138+80\log_{10}M_h+0.9\,\alpha^\circ_{0.85}\text{dB}$$

where M_h here denotes the blade helical tip Mach number. The major part of this noise arises from the harmonic tones of the blade-passing frequency. However, there is an increase in

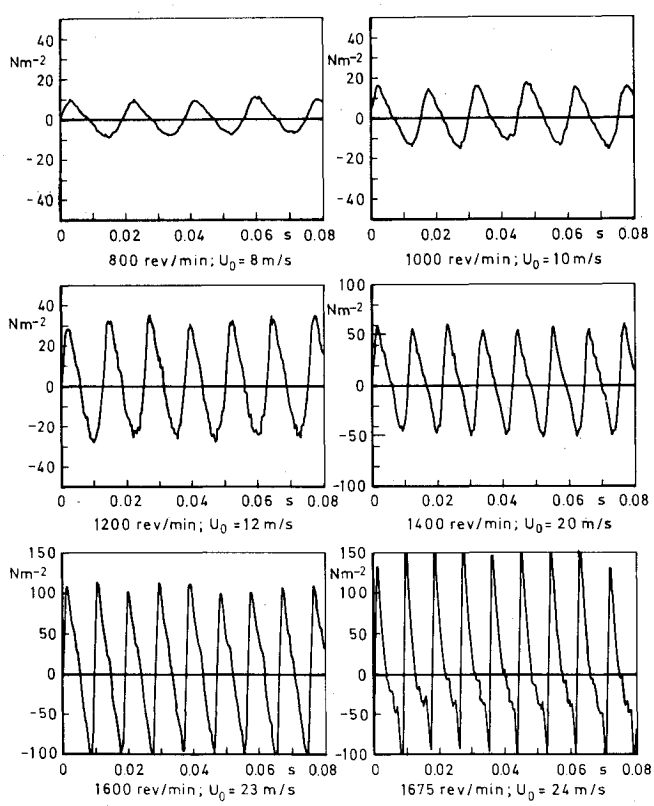

Fig. 3 Time histories—near field. $\beta_{0.7}=21.5$ deg; $U_{\text{nom}}=0$; $r/R=1.44$; $\theta=90$ deg.

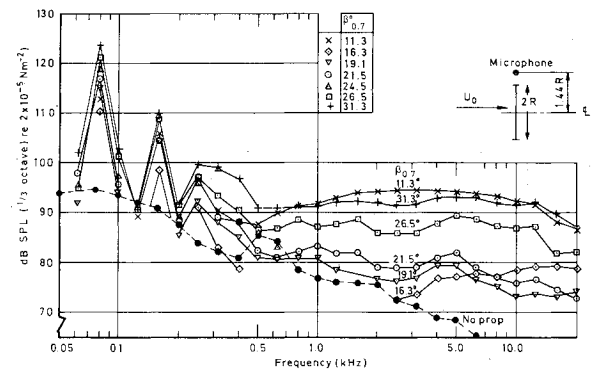

Fig. 4 1200 rpm; $U_0=30$ m/s; $r/R=1.44$—near field (full-scale propeller in a 24-ft tunnel).

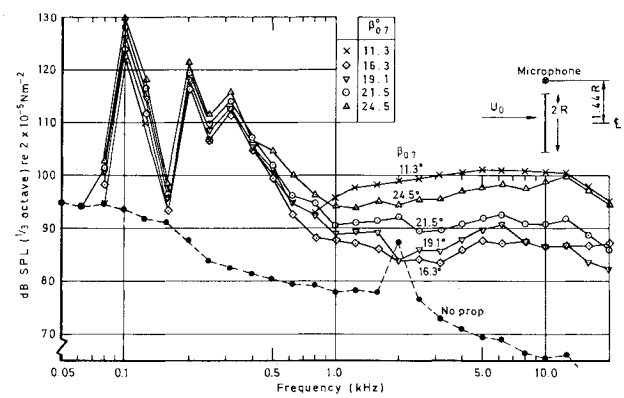

Fig. 5 1600 rpm; $U_0=30$ m/s; $r/R=1.44$—near field (full-scale propeller in a 24-ft tunnel).

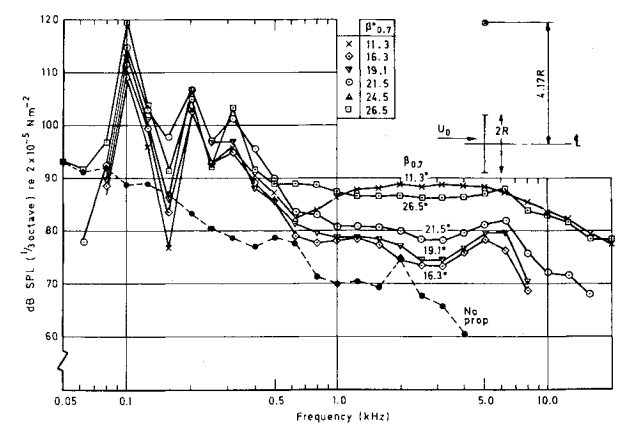

Fig. 6 1600 rpm; $U_0=30$ m/s; $r/R=4.18$—far field (full-scale propeller in a 24-ft tunnel).

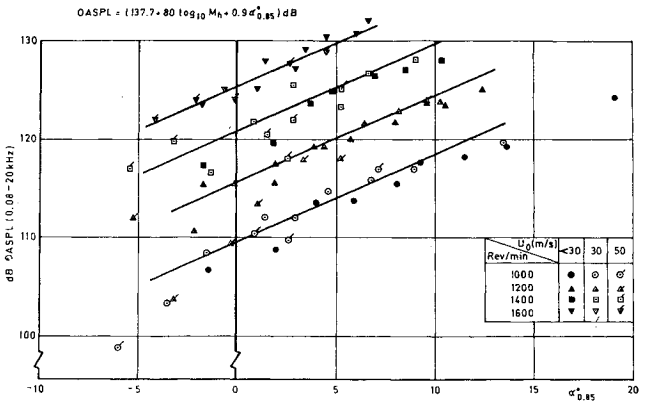

Fig. 7 Variation of OASPL of full-scale propeller with blade incidence and rotational speed ($r/R = 1.44$).

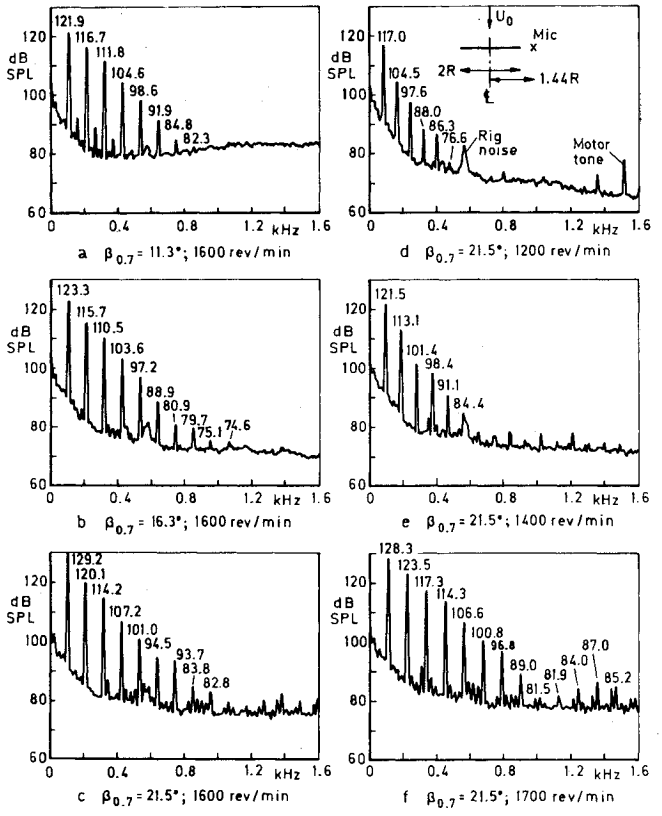

Fig. 8 $r/R = 1.44$; $\theta = 90$ deg; $U_0 = 30$ m/s; narrow-band spectra (full-scale propeller in a 24-ft tunnel).

broadband noise content at high frequencies when the propeller is lightly loaded (e.g., $\beta_{0.7} = 11.3$ deg on Figs. 5 and 6).

The selection of narrow-band frequency spectra is here limited to sufficient conditions to indicate broad trends in noise levels as the propeller parameters are varied though many more spectra have been analyzed. Noise spectra for the frequency range 0-1.6 kHz are presented for the near-field microphone ($r/R = 1.44$) in Fig. 8 and for the far-field microphone ($r/R = 4.17$) in Fig. 9; the numerical values of the SPL for the blade-passing frequency and its harmonics are indicated. The effect of increasing the blade setting at constant rotational speed can be gaged by comparing the diagrams a, b, and c of each figure. Similarly, the effect of increase in rotational speed at constant blade setting can be studied by comparing the related diagrams d, e, c, and f.

As is to be expected, the highest value of SPL normally occurs at the blade-passing frequency but significant tones also persist at multiple harmonics of that frequency. The

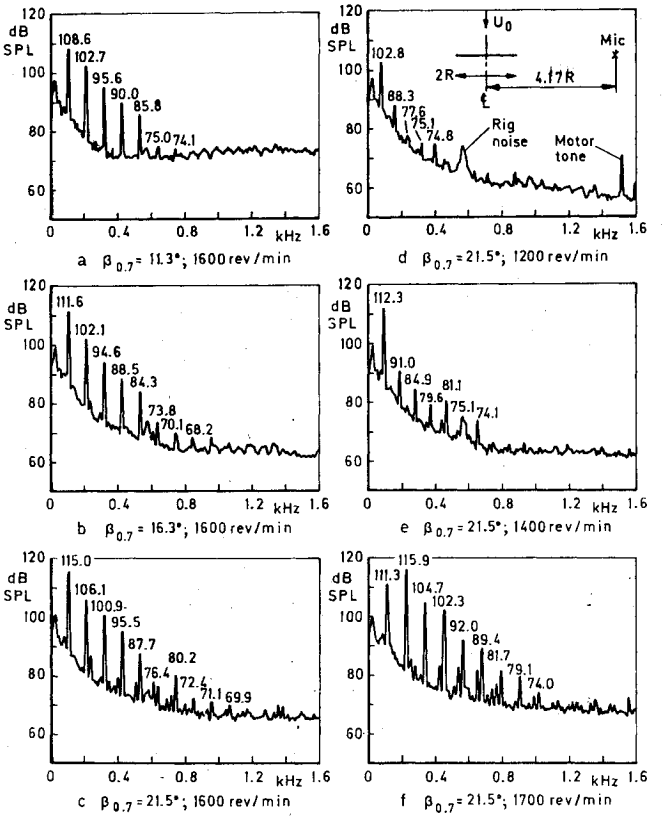

Fig. 9 $r/R = 4.17$; $\theta = 90$ deg; $U_0 = 30$ m/s; narrow-band spectra (full-scale propeller in a 24-ft tunnel).

number of measurable harmonic tones increases with propeller speed and this is consistent with the steepening of the pressure response curve observed earlier (Fig. 3). In general, the SPL of the fundamental tone rises with both propeller blade setting angle and with rotational speed (i.e., increased torque and thrust), except that there is a reduction in level of 1 or 2 dB when the propeller speed is raised from 1600 to 1700 rpm. However, this latter reduction is accompanied by substantial increases in the other harmonics and so there remains an increase in the OASPL at the higher speed.

The effects of variations in the power absorption and rotational speed on the strength of the SPL of the blade-passing-frequency tone can be studied for the near-field microphone. The signal intensity I is found to be proportional to the square of the power coefficient C_p ($=\text{power}/\rho n^3 D_p^5$) throughout the propeller speed range 800-1700 rpm, and to the eighth power of blade-tip speed V_{tip} ($=\pi nD$) within the more limited range 1000-1600 rpm. It is also shown in Fig. 10 that the mainstream Mach number (M_0) as well as blade-tip helical Mach number M_h has a significant effect; and the SPL of the fundamental tones can be correlated by the following expression:

$$\text{SPL} = 162 + 10 \log_{10} (M_h^8 C_p^2) - 40 M_0$$

A similar correlation expression had also been obtained for five-bladed propellers suitable for this aircraft. Figure 10a shows that this formula gives full-scale propeller noise levels at the near-field microphone within 2 or 3 dB of the measured values over the range of parameters of practical interest.

Later analysis has shown that a similar relation could be applied for noise at the fuselage-mounted microphones used during flight research on the twin-propeller Shorts 330 aircraft. Naturally, installation effects and the presence of a second propeller here increased the noise level, with the result that the constant in the parametric expression has to be in-

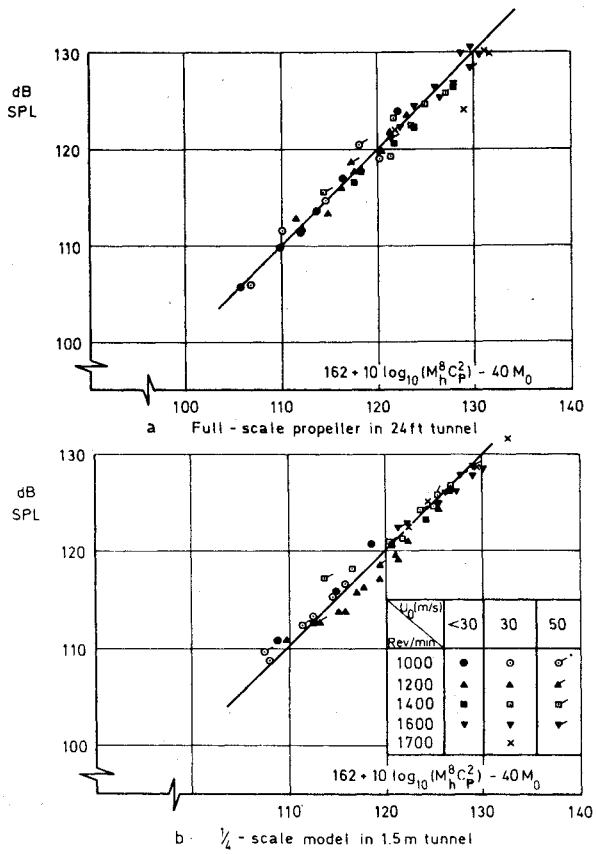

Fig. 10 Sound pressure level of blade-passing frequency; $r/R = 1.44$—near field.

creased by some 7 dB to 169. Much of this excess noise would, of course, arise from reflections off the nearby fuselage side.

It may be added that 10 deg changes in propagation direction or propeller axis attitude had no significant effect on noise characteristics with this particular propeller.

Comparison of Characteristics of Quarter-Scale Model with Full-Scale Model

Range of Model Aeroacoustic Experiment

Investigations with the quarter-scale propeller in the 1.5-m acoustic tunnel have been made over the wide blade-angle setting range $\beta_{0.7} = 10$-45 deg at airspeeds between 0 (nominal) and 50 m/s. As with the full-scale propeller, the minimum airspeed ($U_{nom} = 0$) was that induced in the tunnel solely by the propeller slipstream, though the added constriction in the circuit of the 1.5-m tunnel did result in somewhat lower minimum airspeeds than those experienced with the full-scale propeller in the 24-ft tunnel. Naturally, on the model the rotational speed had to be increased by a factor of 4 over that for the full-scale propeller to give the same blade-tip speed.

Propeller Aerodynamic Performance

From the power and thrust measurements made on each propeller at various blade settings between $\beta_{0.7} = 10$ and 45 deg, the power coefficient ($C_p = \text{power}/\rho n^3 D^5$) and thrust coefficient ($C_T = \text{thrust}/\rho n^2 D^4$) have been derived as functions of the advance factor ($J = U_0/nD$) for mainstream airspeeds of 30 and 50 m/s, respectively. Here, in Fig. 11, interpolated values are cross-plotted against blade setting for J values of 0.4, 0.8, and 1.2. These results indicate generally good agreement between the model- and full-scale propeller, though there is some discrepancy (of the order of 1 deg in blade setting) under low loading conditions at $J = 1.2$ (i.e., when $C_p < 0.1$). Of further significance is the observed increase in both C_p and C_T when the mainstream speed is raised

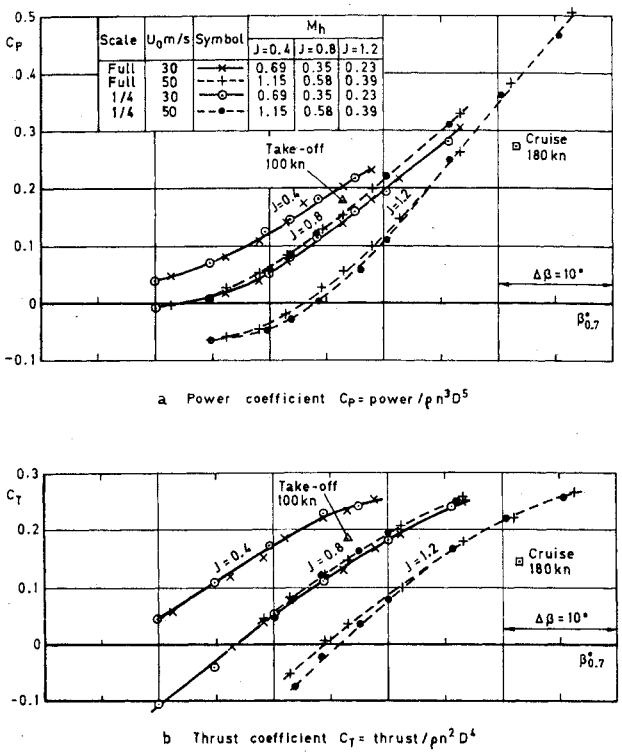

Fig. 11 Performance comparison between model- and full-scale propeller.

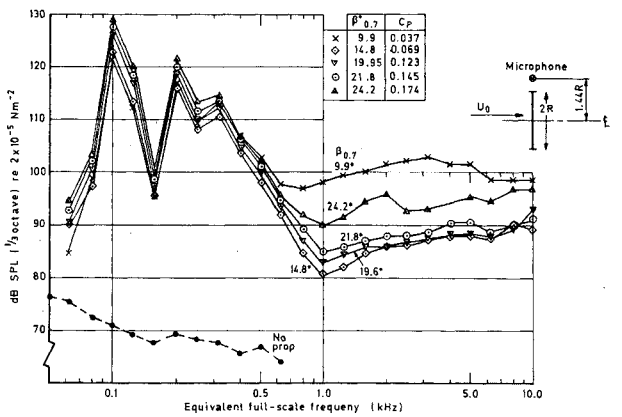

Fig. 12 One-third-octave spectra for ¼-scale propeller in a 1.5-m tunnel. 6400 rpm; $U_0 = 30$ m/s; $r/R = 1.44$.

from 30 to 50 m/s, here illustrated for $J = 0.8$. Identical trends, observed for both model- and full-scale propellers, presumably result from the fact that a higher rotational speed (and hence higher blade-tip Mach number) is required at the greater airstream speed to maintain the same value of J. This implies that, at least for the highly loaded conditions, it is preferable to make performance investigations at the correct Mach number even though this may entail model testing at a reduced scale in order to make the tests in a facility with a suitable speed range.

Propeller Noise Characteristics

Typical one-third-octave spectra for the model at 6400 rpm (Fig. 12) show very similar trends to the corresponding full-scale results at 1600 rpm (Fig. 5), though the blade settings differ slightly for the two propellers. Moreover, both propellers exhibit the phenomenon of a rise in the high-frequency content of the broadband noise levels at low blade setting (i.e., when the propeller is lightly loaded). The spectra can be compared usefully at a constant Strouhal number

($S = fD_p/V_{tip}$) for nearly identical blade settings, e.g., for $\beta_{0.7} = 21.5$ deg in Fig. 13. Here the blade-passing frequency for the four-bladed propeller occurs at $S = 4/\pi$. The comparisons made at equivalent full-scale frequencies of 1200 and 1600 rpm show good agreement in the spectra except in the range $5 < S < 20$. To some extent the discrepancy in this region is attributable to the intrusion of tunnel background noise in the 24-ft tunnel tests, particularly at the lower rotational speed of 1200 rpm; but the high turbulence level in the 24-ft tunnel (0.5%) as against 0.25% may also be adversely affecting propeller broadband noise at frequencies below 2 or 3 kHz. There is some supportive evidence of this effect from some recent acoustic research on helicopter rotors and confirmation may be possible from further investigation with the model propeller by varying the turbulence level of the mainstream flow in the 1.5-m tunnel.

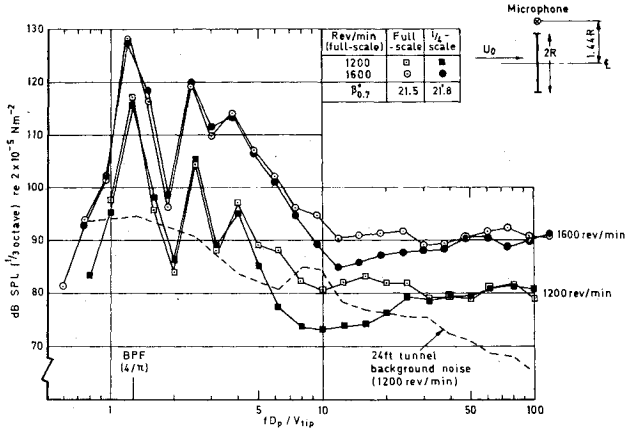

Fig. 13 Comparison of noise spectra of model- and full-scale propellers. $U_0 = 30$ m/s; $r/R = 1.44$.

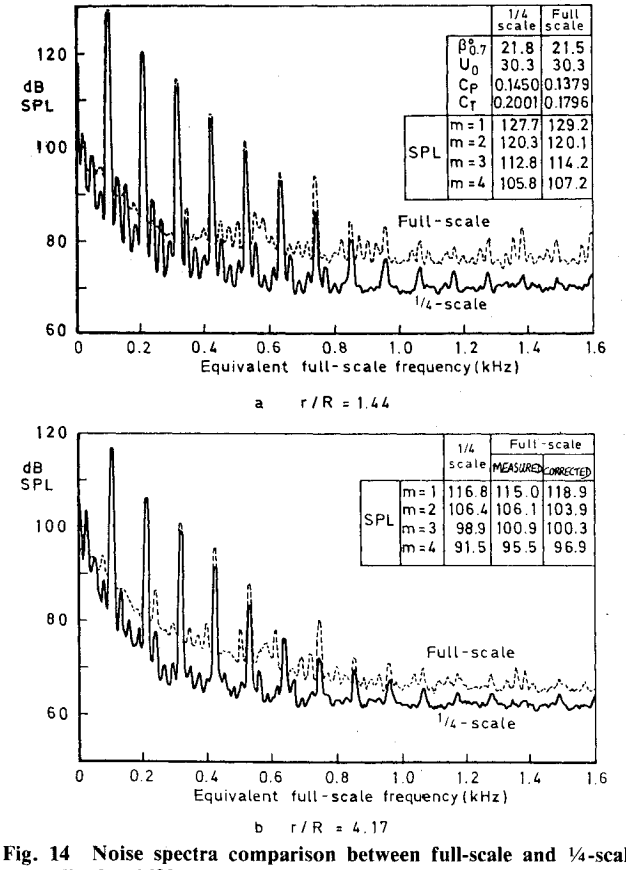

Fig. 14 Noise spectra comparison between full-scale and ¼-scale normalized to 1600 rpm; $U_{nom} = 30$ m/s.

Typical comparisons of narrowband spectra for the model- and full-scale propellers are shown in Fig. 14 at both near- and far-field microphones, with a tunnel airspeed of 30 m/s. Again, a blade setting of $\alpha_{0.7} = 21.5$ deg is chosen and the spectra at equivalent full-scale rotational speeds of 1200 and 1600 rpm are illustrated. For the near-field microphone ($r/R = 1.44$) there is a good correlation between the measured value of the sound pressure levels of the various tonal harmonics in the spectra, particularly at the higher rotational speeds, though again the broadband noise is noticeably larger for the full-scale propeller. The advantages to be gained from model testing in the quieter 1.5-m acoustic tunnel are clearly demonstrated in Fig. 15; even at an equivalent rotational speed as low as 1000 rpm and the high tunnel speed of 50 m/s, there is little contamination of the model-propeller noise signal by the 1.5-m tunnel background noise though the corresponding full-scale propeller noise was completely swamped by the background noise in the 24-ft tunnel. Values of the SPL for the model propeller at the blade-passing frequency, derived from measurements over a large range of blade setting and airspeed, have been plotted in Fig. 10b against the parametric formula

$$162 + 10\log_{10}(M_h^8 C_p^2) - 40M_0$$

derived earlier for the full-scale propeller (Fig. 10a). On this basis of correlation there is very good agreement between the results for the model- and full-scale propellers at appropriately scaled distances.

Corresponding comparisons of the far-field noise measurements ($r/R = 4.17$) are complicated by the effects of reflections from the acoustic curtain in the 24-ft tunnel. As discussed earlier, a simple correction formula has been deduced for the effect of this reflection on the SPL of the tones for the full-scale propeller, and Fig. 14 lists both measured and corrected values of SPL. Broadly speaking, application of the correction gives better agreement between the results for the full- and quarter-scale propellers. Certainly the model-scale results appear to be far more orderly than the uncorrected measured values for the full-scale propeller.

Correlation Between Theoretical Predictions and Experimental Results

Far-Field Noise

While the aforementioned empirical parametric formulas offer simple useful tools to indicate practical trends and to

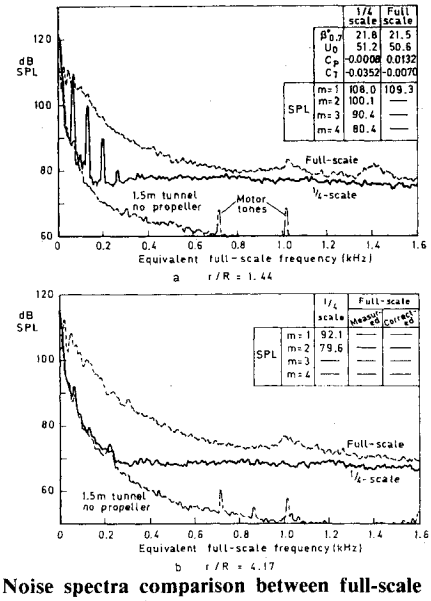

Fig. 15 Noise spectra comparison between full-scale and ¼-scale normalized to 1000 rpm; $U_{nom} = 50$ m/s.

isolate unusual conditions quickly, they cannot be expected to ensure reliable clarification of primary noise sources and their changes with test condition, for which we must provide well-defined theoretical frameworks with experimentally justified elements. Typical, measured third-octave spectra for the noise far-field ($r/R = 4.17$, $\theta = 90$ deg) from 24-ft tunnel tests on the full-scale Dowty-Rotol propeller are compared with combined loading plus broadband noise predictions (Magliozzi, 1976) in Fig. 16. The measured tone levels are compared with the predictions of separate elements from steady loading (Garrick and Watkins, 1954), unsteady loading (Lowson and Ollerhead, 1969), and thickness (Succi, 1979/Hawkings, 1975) in Fig. 17.

Clearly the predicted tone at blade-passing frequency (BPF) is dominated by the steady-loading contribution (Garrick and Watkins), though this prediction can be several dB below the measured tone. The $2 \times$ BPF tone is predicted to contain contributions of importance from both the steady-loading and thickness source (Hawkings/Succi), and the combined predicted intensity may even just exceed the measured tone, except at low rotational speeds where the tone becomes submerged in the propeller-broadband or tunnel-background noise contributions. The predictions for the $3 \times$ BPF and $4 \times$ BPF tones are usually dominated by the thickness-noise contribution except, again, at low rotational speeds. The unsteady-loading predictions only become significant for the harmonics from $5 \times$ BPF upwards, when the predicted values are near to the measured values at low blade angles but fall well below at high blade angles. Presumably these latter tend to be reduced further (by several dB) if Magliozzi's new evaluation (1979) for the unsteady-loading harmonics is adopted, corresponding to uninstalled rather than installed propeller characteristics. Moreover, his current choice of static conditions as a datum for this unsteady-loading treatment cannot be accepted as reliable, even if of practical necessity at this time; because gross reductions to the resulting SPL estimates then have to be applied to allow for the substantial removal of ingested turbulence when airspeed is raised to 10 knots or beyond.

The broadband noise contributions from the Magliozzi empirical formula usually dominate the predicted third-octave spectra at frequencies above $4 \times$ BPF. However, even with an arbitrary reduction of 10 dB in the predicted level of the broadband noise, the correspondingly reduced estimates for the associated third-octave spectra contributions around 1 kHz give levels still up to 6 dB higher than the measured values. Admittedly at very high frequencies (above 5 kHz), the number and amplitude of predicted unsteady-loading harmonics can raise the effective third-octave levels there.

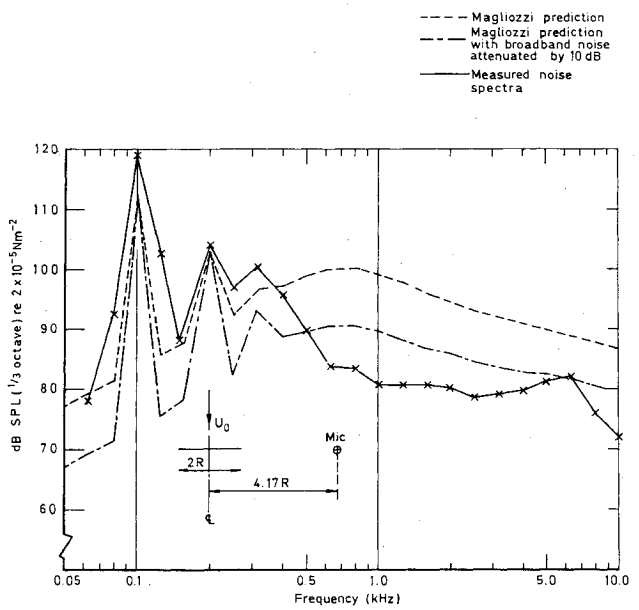

Fig. 16 Comparison of measured third-octave spectra with Magliozzi-type predictions. $\beta_{0.7} = 21.5$ deg; 1600 rpm; $U_0 = 30$ m/s; $\theta = 90$ deg; $r/R = 4.17$—far field.

Near-Field Noise

The near-field version of Garrick and Watkins development of Gutin's theory, to cover forward-speed conditions for rotational steady-loading noise only, has in the past provided the main method for near-field noise prediction. But its practical accuracy has so far been uncertain owing to lack of sufficient supporting test data. Typical measured tone levels from 24-ft tunnel tests on the full-scale Dowty-Rotol propeller in the near-field ($r/R = 1.44$, $\theta = 90$ deg) can be compared in Fig. 18 not only with the predictions of separate elements from steady-loading (Watkins and Durling) but also with thickness effects (Succi) as outlined earlier.

The predicted BPF tone is again usually dominated by the steady-loading contribution, being roughly equal to or at most 3 dB below the measured values. The $2 \times$ BPF prediction can exhibit more or less equal contributions from steady-loading and thickness sources, but for the higher harmonics the thickness contribution dominates. Overall, the predicted tone levels up to $6 \times$ BPF agree remarkably well with the measured noise values. The shortfall of the predictions at higher frequencies may possibly be associated with the intrusion of tunnel-background or test-rig noise rather than true propeller noise, and this should be further explored. The unimportance of unsteady-loading effects on the near-field noise of isolated propellers seems to be confirmed, but at this stage their possible significance in practical airframe installations must be kept in mind.

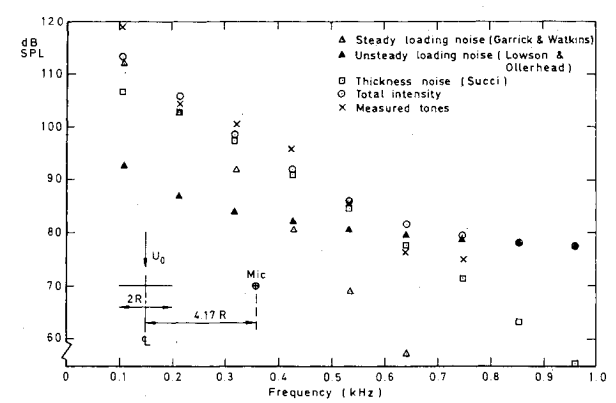

Fig. 17 Comparison of measured tones with predicted elements. $\beta_{0.7} = 21.5$ deg; 1600 rpm; $U_0 = 30$ m/s; $\theta = 90$ deg; $r/R = 4.17$—far field.

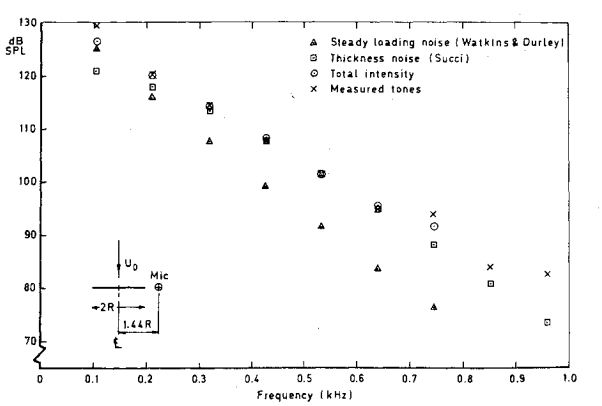

Fig. 18 Comparison of measured tones with predicted elements. $\beta_{0.7} = 21.5$ deg; 1600 rpm; $U_0 = 30$ m/s; $\theta = 90$ deg; $r/R = 1.44$—near field.

Concluding Remarks

The foregoing aeroacoustic analysis of a modern full-scale propeller for wind tunnel speeds up to 50 m/s, variations of blade rotational speed up to helical tip Mach number M_h of 0.75, and extensive coverage of the practical range of blade-angle settings (blade aerodynamic incidence), clearly demonstrates the predominance of multiple tones whose number grows with increasing M_h in both the far and near field. The empirical formula derived for the near-field SPL at blade-passing frequency forcibly illustrates the significance of aerodynamic power coefficient (C_p) and M_h, and confirms the anticipated reduction in noise level with increasing mainstream speed away from near-static conditions.

The quarter-scale model propeller is shown to have aerodynamic performance characteristics encouragingly close to full-scale, while the noise spectra generally agree at the appropriate scale frequency (same Strouhal number), and a similar empirical relationship holds for the SPL at blade-passing frequency. Furthermore, the advantages to be gained from model testing in the quieter 1.5-m tunnel are clearly demonstrated. Even at blade-tip Mach number as low as 0.5 and mainstream speed as high as 50 m/s, there is little contamination of the propeller signal by tunnel background noise, though the full-scale propeller signal is completely swamped by background noise under these extreme conditions in the 24-ft tunnel.

The theoretical framework adopted for far-field noise prediction contains conventional elements from rotational steady loading (Garrick and Watkins), unsteady loading (Lowson and Ollerhead), and broadband noise (semiempirical). For convenience, these contributions have been evaluated using computer programs published by Magliozzi, though the actual blade geometry and measured values of the thrust are taken here rather than theoretical estimates. When supplemented by thickness noise estimates (Hawkings or Succi), the tonal contents of the predicted acoustic signals agree reasonably well with measured values. But the particular predictions of broadband noise using the Magliozzi formulas (1976) can be as much as from 10 to 15 dB more than the measured values.

The theoretical framework for near-field prediction contains again the effects of rotational steady loading, but of necessity introduces a more complex calculation procedure (Watkins and Durling) than that accepted previously for far-field noise computations. Here, when supplemented by thickness noise estimates (Succi), the predicted tonal contents agree remarkably with the measured values.

References

[1] Williams, J. and Trebble, W.J.G., "Some British Research on Propeller Noise Characteristics Under Low-Speed Wind-Tunnel and Aircraft Flight Conditions," RAE Technical Memorandum Aero 1843, Royal Aircraft Establishment, Farnborough, Hants, England 1980.

[2] Amiet, B.K., "Corrections of Open Jet Wind Tunnel Measurements for Shear Layer Refraction," AIAA Paper 75-532, 1975.